



Co-detection: Ultra-reliable nanoparticle-based electrical detection of biomolecules in the presence of large background interference

Yang Liu^{a,b,*}, Ming Gu^c, Evangelyn C. Alcocilja^d, Shantanu Chakrabarty^c

^a Department of Civil and Environmental Engineering, The University of Michigan, USA

^b Department of Electrical Engineering and Computer Science, The University of Michigan, USA

^c Department of Electrical and Computer Engineering, Michigan State University, 2120 Engineering Building, East Lansing, MI 48824, USA

^d Department of Biosystems and Agricultural Engineering, Michigan State University, 115 Farrell Hall, East Lansing, MI 48824, USA

ARTICLE INFO

Article history:

Received 14 June 2010

Received in revised form 18 August 2010

Accepted 20 August 2010

Keywords:

Biomolecules

Co-detection

Biosensor

Forward error-correction biosensor

Electrical detection

Biomolecular circuits

ABSTRACT

An ultra-reliable technique for detecting trace quantities of biomolecules is reported. The technique called “co-detection” exploits the non-linear redundancy amongst synthetically patterned biomolecular logic circuits for deciphering the presence or absence of target biomolecules in a sample. In this paper, we verify the “co-detection” principle on gold-nanoparticle-based conductimetric soft-logic circuits which use a silver-enhancement technique for signal amplification. Using co-detection, we have been able to demonstrate a great improvement in the reliability of detecting mouse IgG at concentration levels that are 10^5 lower than the concentration of rabbit IgG which serves as background interference.

© 2010 Elsevier B.V. All rights reserved.

1. Introduction

A major challenge in the area of biosensors is to be able to detect target biomolecules in the presence of large background interference (Draghici et al., 2005). In many cases, background interference could simply constitute the presence of non-target analytes which could not only produce non-specific binding events but also cause steric hindrance, preventing binding between target analytes with its specific recognition probes (antibody or DNA) (Marshall, 2004). Most of the reported methods in biosensors either aim to reduce the effect of background interference using pre-filtering techniques (Wang et al., 2005) or aim to boost the concentration of the target analyte using pre-concentration (Fitch et al., 2003) or target-amplification (e.g. polymerase chain reaction or PCR) (Huse et al., 2007; Noonan et al., 2006). In this paper we report that background interference created by the presence of non-specific analytes can be exploited to amplify and improve the reliability of detection of the target analyte. The technique is based on our previously reported

forward error-correction (FEC) biosensor (Liu et al., 2007), which investigates the novel FEC interfaces to biosensors to improve their reliability.

Forward error correction (FEC) is a technology, which is widely used in telecommunication systems, to provide robustness to systems. This allows the receiver to detect and correct errors (within some bound) without the need to ask the sender for additional data. Also, FEC technique is applied to most mass storage devices to protect against damage to the stored data. In the literature, FEC principles have been used for improving reliability of nanoscale systems, which suffer from similar computational artifacts as storage systems. Some of the examples include design of fault-tolerant circuits (Kuekes et al., 2005) and next generation flash memory (Gregori et al., 2003). Other works in related areas include application of the FEC principle for understanding biological systems (Fedichkin et al., 2008; May et al., 2003). For example, error-correcting codes were proposed for a DNA microarray, where redundant gene spotting was used to reduce drop-out errors (Khan et al., 2003). This work was extended in (Milenkovic, 2006) where the error-control coding scheme and quality control were integrated for fabricating DNA microarrays using multiplexed DNA strands.

The key attribute of a FEC biosensor in this work is synthetic encoding and patterning of probes (for e.g. antibodies) into fundamental logic units and the subsequent decoding of signals measured from these units. Similar to methods used in commu-

* Corresponding author at: University of Michigan, Department of Civil and Environmental Engineering, 2314 G.G. Brown Building, Ann Arbor, USA.
Tel.: +1 734 615 8177.

E-mail address: yaliu@umich.edu (Y. Liu).

¹ This research was performed when Dr. Liu was a Ph.D. student at Michigan State University.

nication and storage systems, appropriate encoding and decoding could potentially correct for any errors that occur due to device imperfections or stochastic interactions between biomolecules (for e.g. antigen–antibody interactions). In our prior work, we have demonstrated the functionality of two basic logic units (namely “AND” and “OR” gates) which were fabricated using on a lateral flow immunoassay. However, these logic gates exhibited large variability in their response and substantial leakage that limited the potential of the FEC principle. In this paper, we propose to use a silver-enhancement technique to design, fabricate and validate the functionality of the basic logic units on a gold-nanoparticle-based biochip.

Co-detection is similar in spirit to many noise exploitation techniques like stochastic resonance which has been reported in physics (Almog et al., 2007) and biology (Wiesefeld and Moss, 1995; Russell et al., 1999), where it has been shown that the addition of random noise into a non-linear system in fact improves the system sensitivity. However, the key towards implementing co-detection in biosensors is to effectively control the coupling (or interference) between different analytes and to exploit the non-linear response of the biosensor. In this work, we first report the fabrication of biomolecular logic circuits using silver-enhanced nanoparticles and then use the biosensor platform to demonstrate the “co-detection” principle. We show that the proposed approach can improve the reliability of detecting target analyte (mouse IgG) by three orders of magnitude when the background interference (rabbit IgG concentration) is more than 10^5 higher than the target analyte (mouse IgG) concentration.

2. Materials and methods

2.1. Biochip fabrication

We fabricated biomolecular logic gates on a silver-enhanced gold-nanoparticle-based biochip and the “co-detection” principle is also demonstrated on the biochip. The following procedure was used for fabricating the silver-enhanced gold-nanoparticle-based biochip and then immobilizing specific antibodies onto the substrate. The biochips were fabricated from to 4" (100) silicon wafers (thickness 500–550 μm). A 2 μm thick layer of thermal oxide was grown over the silicon to serve as an insulator between the electrodes and the substrate. Photolithography was used to pattern photo-resist (PR) followed by deposition of metal electrodes through evaporation of 10 nm of chrome under 100 nm of gold and the formation of an interdigitated electrode array (IEA) using a lift-off process.

2.2. Biochip surface functionalization

The surface of biochips was then modified for immobilizing the antibody. The chips were first immersed in acetone in a crystallizing dish for 10 min to dissolve away the protective PR layer. The chips were then treated with 1:1 mixture of concentrated methanol and hydrochloric acid for 30 min followed by immersion into boiling distilled water for 30 min. The biochips were allowed to air dry completely. The biochips were then silanized in an anaerobic glove box. The biochips were immersed in a crystallizing dish containing a solution of 2% 3-Mercaptopropyltrimethyloxysilane (MTS) (Sigma; St. Louis, MS) for 2 h. The chips were then rinsed in toluene and were allowed to dry completely. After silanization, N- γ -maleimidobutyryloxy succinimide ester (GMBS) (Sigma; St. Louis, MA) was chosen as crosslinkers to avoid formation of multi-protein complex. The crosslinking reagent was dissolved in a minimum amount of dimethylformamide (DMF) and then diluted with ethanol to a final concentration of 2 mM. The silanized sub-

strate was treated with crosslinker for 1 h and washed in phosphate buffered saline (PBS, pH 7.4). After the application of the crosslinker, antibody (Sigma; St. Louis, MA) was immobilized onto the biochip active surface. The biochips were placed in a petri dish, sealed with parafilm and allowed to incubate at 37 °C for 1 h. The biochips were then treated with 2 mg/mL bovine serum albumin (BSA) (Sigma; St. Louis, MA) for 45 min. After incubation, the biochip surface was rinsed with PBS (pH 7.4) and was allowed to air dry (summarized in Supplementary Fig. 2).

3. Results and discussion

The principle which we call “co-detection” can simply be illustrated using a biosensor reliability curve in Fig. 1a where analyte 1 serves as the target to be detected and analyte 2 serves as the background interference. Ideally, the detection error-rate (DER) or the sum of false-positive or false-negative errors decreases with the increase in analyte 1 concentration (ignoring the Hook effect; Selby, 1999) and the DER is largely unaffected or increases when the concentration of analyte 2 (acting as background interference) increases. However in “co-detection”, addition of analyte 2 reduces the DER for analyte 1, as illustrated in Fig. 1a, and hence enhances the reliability of detection.

The architecture of the two logic functions (soft-AND and soft-OR) which has been used in this work is shown in Fig. 1b and g where antibodies corresponding to analyte A and B (mouse IgG and rabbit IgG) are patterned at different spatial locations between two gold electrodes. For the soft-OR logic gate, a mixture of goat anti-rabbit IgG and goat anti-mouse IgG was patterned as shown in Fig. 1b, where as for the soft-AND gate, the antibodies were patterned in a cascaded fashion as shown in Fig. 1g (Supplementary Fig. 1).

When the analyte is applied to the immobilized biochips, the target biomolecules (mouse and rabbit IgG) hybridize with their specific antibodies. The secondary antibodies conjugated with gold (Au) nanoparticles are then applied to the biochip, which leads to the formation of a sandwich assay as shown in Fig. 1c. In this stage, the current measured between the electrodes (for a fixed potential difference) is small. The next step involves a silver-enhancement technique to amplify the hybridization events into a measurable electrical signal. The sandwich assay is exposed to a solution of Ag(I) and hydroquinone (photographic developing solution). The gold nanoparticles act as a catalyst and reduce silver ions into metallic silver in the presence of a reducing agent (hydroquinone). The reduced silver then deposits on the gold surface, thus enlarging the size of the gold nanoparticles as shown in Fig. 1d. As the size of the silver islands grows, they provide shorter paths for electrons to hop between the electrodes. With the increase in enhancement time (the time of the exposure with the silver enhancer solution), the consistent growth of silver-enhanced particles completely bridges the area between the electrodes (shown in Fig. 1d). Even though, silver-enhancement technique has been used for conductometric DNA arrays and immunoassays (Park et al., 2002; Velev and Kaler, 1999; Gupta et al., 2007; Shyu, 2002; Liao and Huang, 2005), it has not been yet extended to implement logic functions as is reported in this work. In the case of the soft-OR gate the conductive bridge between the electrodes is formed when either one of the analytes (rabbit IgG or mouse IgG) is present in the sample, assuming that the density of antibody probes is large enough. This scenario is shown in Fig. 1d for the case when both rabbit IgG and mouse IgG are present in the sample and Fig. 1f shows an SEM verification of the bridge formation between the two electrodes. Fig. 1e shows the measured conductance across the electrodes during the process of silver enhancement under different logic conditions (control, only mouse IgG present, only rabbit IgG present and both mouse and rabbit IgG present). Please note that the measured conductance

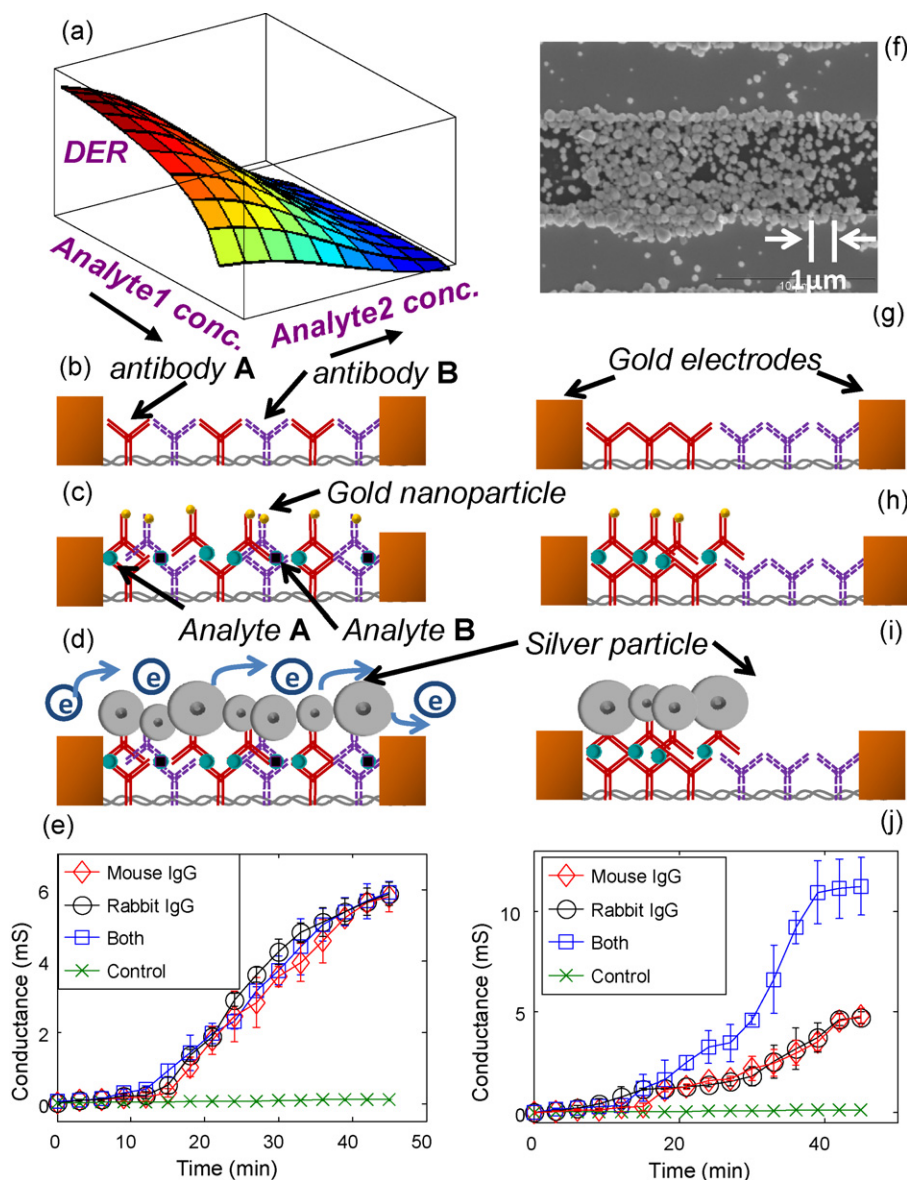


Fig. 1. (a) Illustration of “co-detection” principle, where the presence of analyte 2 enhances the reliability of detection of analyte 1; (b) architecture of an OR gate where the anti-mouse IgG and anti-rabbit IgG are mixed and patterned between the electrodes; (c) formation of a sandwich assay between the target analyte, its specific antibody and a secondary antibody conjugated with gold nanoparticle; (d) silver-enhancement procedure where the gold nanoparticle catalyzes the silver which deposits around the particle, thus increasing its size and in the process forming a conductive bridge between the electrodes; (e) conductance measured across the electrodes of the OR gate during the enhancement procedure (exposure time to Ag enhancement) for different logic conditions; (f) SEM image of the inter-electrode spacing showing the formation of the conductive bridge by silver-enhanced gold nanoparticle; (g) architecture of an AND gate where the anti-mouse IgG and anti-rabbit IgG are cascaded between the electrodes; (h) and (i) formation of partial sandwich assay and conductive bridge due to the presence of only one of the analyte; (j) conductance measured across the electrodes of the AND gate during the silver-enhancement procedure under different logic conditions.

will reach steady state after 40 min. The figure shows that indeed compared to the control experiment, the conductance change is significantly large for all the logic conditions and increases with increase in enhancement time.

In the case of ideal AND gate (shown in Fig. 1g), the bridge across the electrode will be completely formed only when both of biomolecules (rabbit IgG and mouse IgG) are present. However, for a soft-AND gate, the bridge can be partially formed (shown in Fig. 1h and i) when only one of the analytes is present. This leads a smaller conductance change compared to the completely formed bridge. Fig. 1j shows the conductance measured across the electrodes of the AND gate under different logic conditions (control, only one analyte present and both analyte present). The result shows that the change in conductance is the largest when both of biomolecules are present as compared to the condition when only one of the biomolecule is

present, thus verifying the soft-AND logic function. Also, similar to the OR gate response, the conductance increases with increase in enhancement time.

We have also verified that the responses of the fabricated soft-AND and soft-OR gates are consistent across different concentrations of the input analytes. Fig. 2a and b shows the conductance measured across both the gates for different concentrations of analytes and under different logic conditions. For this experiment, the rabbit IgG and mouse IgG were serially diluted using PBS to prepare 100-fold dilutions representing IgG concentrations ranging from 12 μg/mL to 0.12 ng/mL. Each of the tests was repeated three times and the results were measured every 3 min after the replacement of new silver enhancer solution onto biochips. “Control” experiments for all the experiments were obtained using bovine IgG. It can be seen from Fig. 2a and b that under different concentration levels

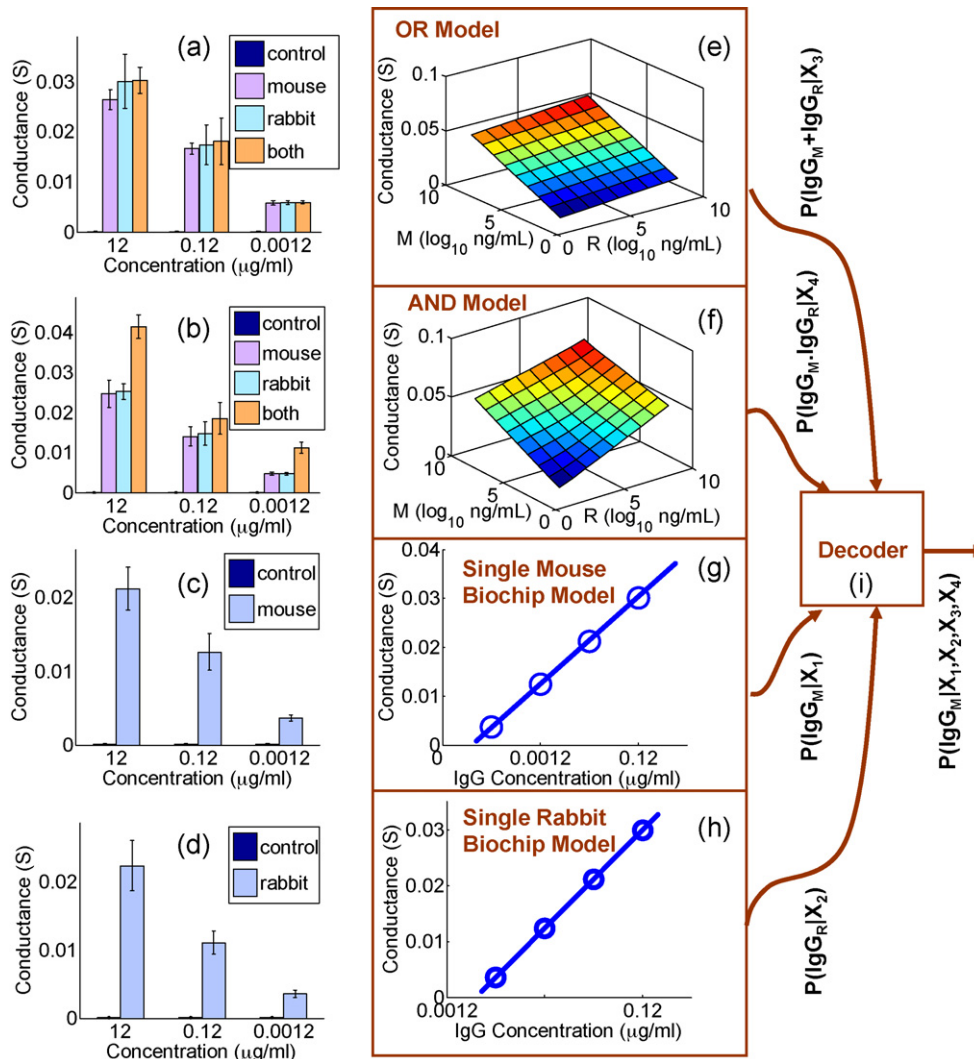


Fig. 2. Experimental results showing the measured conductance from (a) a soft-OR logic gate for different concentration levels of rabbit and mouse IgG; (b) a soft-AND logic gate for different concentration levels of rabbit and mouse IgG; (c) a mouse IgG specific biochip for different concentration levels of mouse IgG; (d) a rabbit IgG specific biochip for different concentration levels of rabbit IgG; coupled log-linear models determined using experimental data for (e) soft-OR logic gate; (f) soft-AND logic gate; (g) mouse IgG biochip; (h) rabbit IgG biochip; (i) architecture of the Bayesian decoder used to compute the posterior probability of the presence of mouse IgG given an array of conductance measurements.

of analytes the response of the logic function remains consistent, however, the magnitude of the measured conductance scales logarithmically with concentration. The measured data was then used to estimate the parameters of a two-dimensional coupled log-linear model (Christensen, 2000), one for each of the logic gates as shown in Fig. 2e and f (Supplementary Fig. 3 and Table 1). Also included in the set of models were single analyte biochips whose measured conductance was only dependent on the concentration of a single analyte (experimental results shown in Fig. 2c and d). The responses of the single analyte biochips are shown in Fig. 2g and h which are one-dimensional log-linear models.

To demonstrate the “co-detection” principle, a total of six different biochips were used: two single analyte biochip specific to mouse IgG, two single analyte biochips specific to rabbit IgG, one soft-AND biochip and one soft-OR biochip (Fig. 3). The experimental procedure involved the following steps: (a) an unknown sample (containing different concentration of mouse and rabbit IgG) were applied to the six biochips; (b) the measured conductance X_i were presented as inputs to the biosensor model, whose outputs were normalized to generate posterior probabilities. For example, the soft-OR biochip model (Fig. 2a) generated the posterior probability $P(IgG_M + IgG_R|X_i)$ that either one of the analytes (rabbit or mouse

IgG) is present given the conductance measurement X_i . As shown in Fig. 2i, all the posterior probabilities are combined together using Bayesian techniques to compute the probability of presence of target analytes $P(IgG_M|X_1, \dots, X_6)$, $P(IgG_R|X_1, \dots, X_6)$ given all the measured conductances X_1, \dots, X_6 (from six biochips) (the decoder is described in Supplementary Figs. 4 and 5) The probability scores are compared against a pre-determined threshold to make a positive identification of the target analyte.

Fig. 4a and b shows the detection error-rate (false-positive error and false-negative error) curves that were obtained by Monte-Carlo simulations using the biochip behavioral models. For this experiment, the magnitude of noise was estimated from the experimentally determined error bars as shown in Fig. 2a–d. In Fig. 4a, the concentration of rabbit IgG is increased which as expected leads to the decrease in its DER. However, the increase in concentration of mouse IgG also leads to the decrease in DER, clearly indicating the “co-detection” principle. A similar behavior was also observed for the DER of mouse IgG as shown in Fig. 4b. For comparison purposes, Fig. 4c shows the DER curves that were obtained if six independent rabbit and mouse IgG biochips are used for detection. This scenario replicates the testing strategy commonly employed in diagnostics where repeated experiments followed by majority vot-

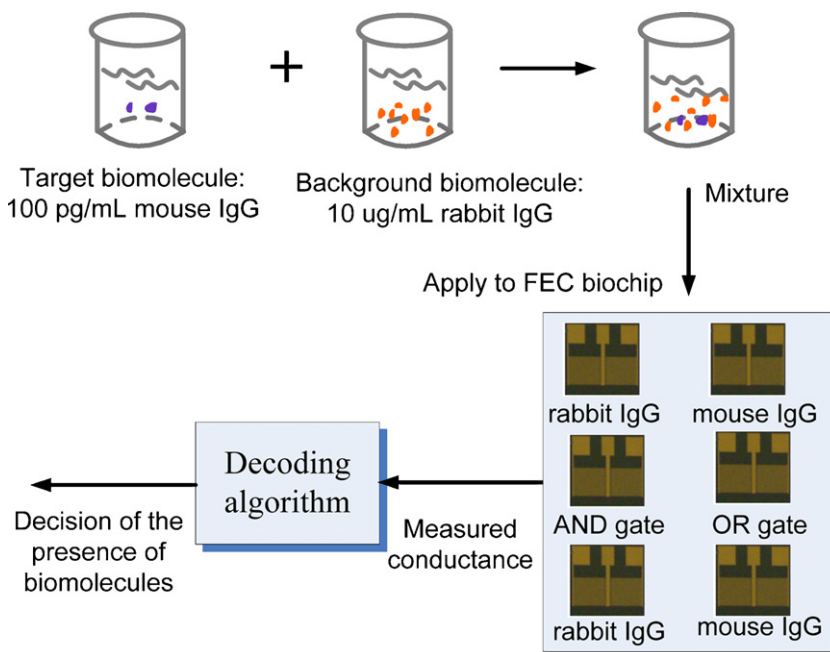


Fig. 3. Experimental setup for verification of the “co-detection” principle.

ing are performed to obtain reliable detection results. The plots in Fig. 4c clearly show the absence of “co-detection” which is expected as there is very little coupling between different detection tests.

We now report results where the “co-detection” principle has been experimentally verified in the detection of mouse IgG. For the experiment, 100 pg/mL mouse IgG is added to the solution of 10 μg/mL rabbit IgG which serves as the background interference. 10 μg/mL bovine IgG is used as negative control experiment. For calibration purposes, we first applied a sample containing

only 100 pg/mL mouse IgG to a single mouse IgG biochip. Fig. 4d shows the detection result compared against the negative control. Even though the experiments show that on average the silver-enhancement technique can detect the trace quantity of mouse IgG, the variance of the experiment (shown by the overlap between the error bars) is too large for reliable confirmation. Fig. 4e shows the result obtained from the single analyte biochip when a mixture of 100 pg/mL mouse IgG and 10 μg/mL rabbit IgG is applied. As expected, the results show similar response as the previous

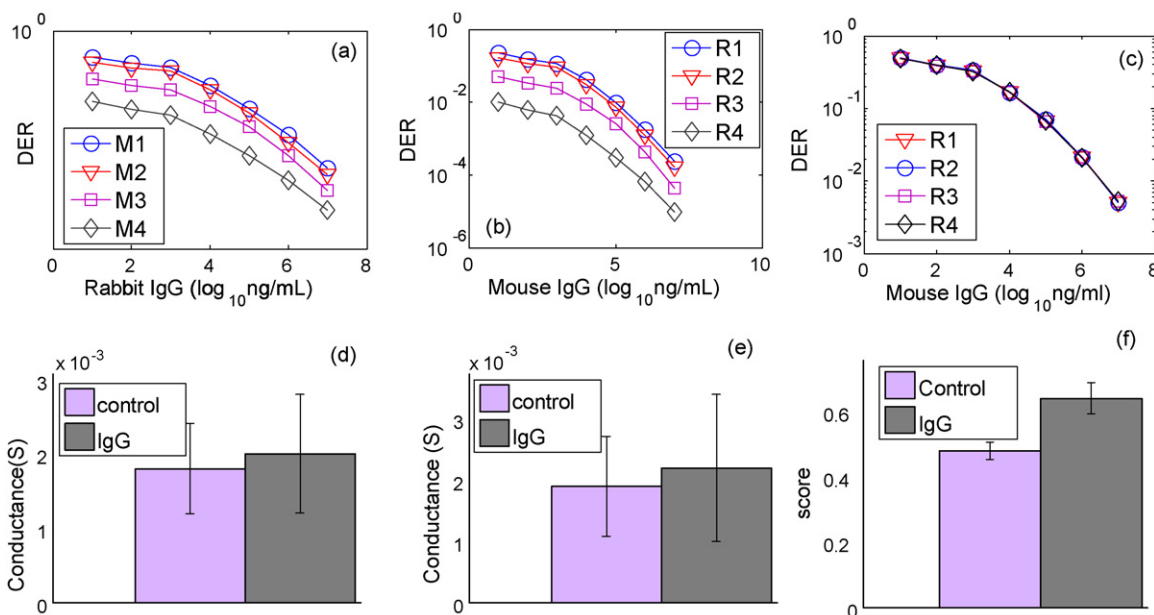


Fig. 4. Demonstration of “co-detection” principle based on mouse IgG experiments and behavioral simulations. Detection error-rate (DER) curves obtained using behavioral models in Fig. 2 for different concentration of rabbit and mouse IgG: (a) showing co-detection when presence of higher concentration of mouse IgG enhances the detection reliability of rabbit IgG. M1 represents mouse IgG concentration: 1 ng/mL; M2 represents mouse IgG concentration: 100 ng/mL; M3 represents mouse IgG concentration: 10 μg/mL; M4 represents mouse IgG concentration: 1 mg/mL. (b) Presence of higher concentration of rabbit IgG enhances the detection reliability of mouse IgG; R1-R4 hold similar meaning and same value as M1-M4. (c) Absence of co-detection in the conventional repetitive tests where rabbit IgG does not affect the detection reliability of mouse IgG; Experimental verification of co-detection: (d) results from a mouse IgG biochip when 100 pg/mL mouse IgG is used; (e) results from a mouse IgG biochip when 100 pg/mL mouse IgG is used in presence of 10 μg/mL of rabbit IgG; (f) results from the Bayesian decoder showing significant improvement in reliability of mouse IgG detection in the presence of background rabbit IgG.

experiment since anti-mouse IgG are non-specific to rabbit IgG. In the last set of experiment, the mixture with similar composition was applied to the six biochips and the measured conductances were processed by the decoding algorithm. Fig. 4f shows the response obtained from the decoder and compares it with results obtained for the negative control experiments (from the experimental setup Fig. 3). Note that the output of the decoder is the normalized score indicating the presence or absence of mouse IgG. It can be clearly seen that not only has the magnitude of the scores increased significantly compared to the control, the variance of the results has also decreased by orders of magnitude. Since there is no overlap between error bars, reliable detection of mouse IgG can be achieved in the presence of high background concentration of rabbit IgG. We believe that the non-linear response of the FEC biochip in conjunction with “co-detection” is the primary reason behind the improvement in reliability. The presence of large background interferences introduces conduction sites which can be easily populated by the target analytes. The computational approach for co-detection bears similarity to DNA signature discovery techniques (Phillippy, 2007). However, the key difference in this work is exploitation of background noise instead of suppressing it. We would also like to point out that even though in our report, we have used only two analytes (mouse IgG and rabbit IgG) to demonstrate the “co-detection” principle, the approach is generic and can be extended to any kinds and any number of analytes. In fact we anticipate significant improvements in reliability as the number of analytes increases. This is because of the exponential increase in the side information that is available through coupling between multiple binding events. One of the key applications where “co-detection” could be used in the future is in the early diagnosis of HIV. Early diagnosis of HIV requires detecting trace quantity of HIV biomolecules that are usually accompanied by other non-specific biomolecules that directly interfere in the detection process (Grant, 2005) and hence require a long-time for confirmation tests. The improvement in reliability offered by “co-detection” will reduce the window period for positive or negative diagnosis and hence can facilitate rapid screening.

4. Conclusions

In this paper, we reported a novel biomolecular detection technique called “co-detection”, which uses background biomolecules as useful information to improve the reliability of detecting target biomolecules. The principle exploits the non-linear coupling amongst synthetically patterned biomolecular logic circuits for deciphering the presence or absence of target biomolecules in a sample. We fabricated a silver-enhanced gold-nanoparticle-based biochip to verify the “co-detection” principle. In this paper we have shown the feasibility of constructing basic logic gates (AND and OR) based on the silver-enhanced gold-nanoparticle-based biochip. AND logic gates have been constructed by cascading two model

anti-IgG, whereas OR logic gates have been fabricated by homogeneously mixing and dispensing of anti-IgG. The biochip utilizes the gold nanoparticle as label and signal transducer in conjunction with specific antigen–antibody binding and it uses silver enhancement as biomolecular level signal amplification.

A major challenge in the area of biosensors is to be able to detect target biomolecules in the presence of large background interference such as in the application of HIV detection. “Co-detection”, however, utilizes the background interference, which is usually regarded as biological noise, as side information to detect target biomolecules. It could be a promising detection technique in the early diagnosis of HIV.

Acknowledgments

This work was supported by a research grant from National Science Foundation: NSF EECS-0622056. The authors thank Lurie Nanofabrication Facility at the University of Michigan for the fabrication of biochips. The authors also would like to thank Professor Rita Colwell from University of Maryland, College Park for their critical comments. Authors would like to thank Xiaowen Liu for the assistance of biochip layout design.

Appendix A. Supplementary data

Supplementary data associated with this article can be found, in the online version, at doi:10.1016/j.bios.2010.08.067.

References

- Almog, R., et al., 2007. *Appl. Phys. Lett.* 90, 013508.
- Christensen, R., 2000. *J. Am. Stat. Assoc.*, 95.
- Draghici, S., Khatra, P., Eklund, A.C., Szallasi, Z., 2005. *Trends Genet.* 22, 101–109.
- Fedichkin, L., Katz, E., Privman, P., 2008. *J. Comput. Theor. Nanosci.* 5, 36–43.
- Fitch, J.P., Raber, E., Imbro, D.R., 2003. *Science* 302, 1350–1354.
- Grant, R.M., 2005. *Science* 30, 2170–2171.
- Gregori, S., Cabrini, A., Khouri, O., Torelli, G., 2003. *Proc. IEEE* 91 (4), 602–616.
- Gupta, S., et al., 2007. *Anal. Chem.* 79, 3810–3820.
- Huse, S.M., et al., 2007. *Genome Biol.* 8, R143.
- Khan, A.H., Ossadtchi, A., Leahy, R.M., Smith, D.J., 2003. *Genomics* 81 (2), 157–165.
- Kuekes, P.J., Robinett, W., Seroussi, G., Williams, R.S., 2005. *Nanotechnology* 16 (6), 869–882.
- Liao, K.T., Huang, H.J., 2005. *Anal. Chim. Acta* 538, 159–164.
- Liu, Y., Chakrabarty, S., Alcocilja, E.C., 2007. *Nanotechnology* 18, 4240107.
- Marshall, E., 2004. *Science* 306, 630–631.
- May, E.E., Johnston, A.M., Hart, W.E., Watson, Pryor, R.J., Rintoul, M.D., 2003. Sandia National Laboratories, SAND Report: 2003–3963.
- Milenkovic, O., 2006. Inaugural Workshop of the Center for Information Theory and Application, San Diego.
- Noonan, J.P., et al., 2006. *Science* 314, 1113–1118.
- Park, S.J., Taton, T.A., Mirkin, C.A., 2002. *Science* 295, 1503–2106.
- Phillippy, A.M., 2007. *PLoS Comput. Biol.* 3 (5).
- Russell, D., Wilkens, L., Moss, F., 1999. *Nature* 402, 219–223.
- Selby, C., 1999. *Ann. Clin. Biochem.* 36, 704–721.
- Shyu, R.H., 2002. *Toxicol.* 40, 255–258.
- Velev, O.D., Kaler, E.W., 1999. *Langmuir*, 15.
- Wang, Y., et al., 2005. *Bioinformatics* 21, 1530–1537.
- Wiesefeld, K., Moss, F., 1995. *Nature* 373, 33–36.